Purdue University Purdue e-Pubs

International Refrigeration and Air Conditioning Conference

School of Mechanical Engineering

2016

Second-Law Analysis to Improve the Energy Efficiency of Environmental Control Unit

Ammar M. Bahman

Ray W. Herrick Laboratories, Purdue University, United States of America, abahman@purdue.edu

Eckhard A. Groll

Ray W. Herrick Laboratories, Purdue University, United States of America, groll@purdue.edu

Follow this and additional works at: http://docs.lib.purdue.edu/iracc

Bahman, Ammar M. and Groll, Eckhard A., "Second-Law Analysis to Improve the Energy Efficiency of Environmental Control Unit" (2016). *International Refrigeration and Air Conditioning Conference*. Paper 1706. http://docs.lib.purdue.edu/iracc/1706

This document has been made available through Purdue e-Pubs, a service of the Purdue University Libraries. Please contact epubs@purdue.edu for additional information.

 $Complete \ proceedings \ may \ be \ acquired \ in \ print \ and \ on \ CD-ROM \ directly \ from \ the \ Ray \ W. \ Herrick \ Laboratories \ at \ https://engineering.purdue.edu/Herrick/Events/orderlit.html$

Second-Law Analysis to Improve the Energy Efficiency of Environmental Control Unit

Ammar M. BAHMAN*1, Eckhard A. GROLL1

¹ Purdue University, School of Mechanical Engineering, Ray W. Herrick Laboratories, West Lafayette, Indiana, USA abahman@purdue.edu, groll@purdue.edu

* Corresponding Author

ABSTRACT

This paper presents a second-law of thermodynamics analysis to quantify the exergy destruction in each component of an Environmental Control Unit (ECU) for military applications. The analysis is also used to identify the potential contribution from each component to improve the overall energy efficiency of the system. Three ECUs were investigated experimentally at high ambient temperature conditions to demonstrate the feasibility of the model presented herein. The investigated ECUs have capacities of 1.5 (5.3 kW), 3 (10.6 kW), and 5 (17.6 kW) tons of refrigeration (RT). The results indicate that the largest potential to improve exergetic efficiency of each unit resides in the compressor. This is followed in order by the evaporator and the condenser in the case of 1.5 RT and 3 RT units, whereas for the 5 RT unit, relatively high irreversibility is associated with the evaporator when compared to the compressor. The second law analysis may help to focus on the components with higher exergy destruction and quantify the extent to which modifying such components can increase the exergetic efficiency of any ECU operating in high ambient temperature environments.

1. INTRODUCTION

Environmental Control Units (ECUs) have been commonly used by the military for space cooling inside shelters in hot climate regions. An ECU is a packaged air conditioner using a conventional vapor compression cycle, whose main components include; a compressor, a condenser, an expansion valve, an evaporator, and a controller. The energy performance of the ECU, typically quantified by the Coefficient of Performance (COP) or the Energy Efficiency Ratio (EER) is evaluated based on the first law of thermodynamics. According to the first law of thermodynamics, energy cannot be created or destroyed. The second law of thermodynamics associates a quality with energy, and can be used to evaluate the degradation in the quality of energy during a process or cycle. Therefore, compared to an energy analysis, the exergy analysis can better detect the location of irreversibilities. The exergetic efficiency of an ECU is a consequence of the destruction of available energy (or exergy) contributed by individual system component. Therefore, a combined first- and second-law analysis directly identifies the components with the potential to improve the efficiency of the ECU. Second-law analyses can be categorized into exergy (or availability) and irreversibility analyses. The former discuss the conversion and loss of exergy while the latter address the entropy generation and irreversibility.

In recent studies, the second-law analysis has increasingly been applied to a variety of heating, ventilating, and air conditioning (HVAC) applications. Bejan (1988) developed an analytical method to conduct second law analyses for thermal systems; whereas Cengel and Boles (2002); Moran et al. (2010); Dincer and Rosen (2015) drafted the second-law analysis for HVAC applications. Fartaj et al. (2004); Xu et al. (2015) studied super-critical CO₂ cycle using second-law analysis. Meunier et al. (1997); Şencan et al. (2005) applied the second-law analysis to absorption and adsorption refrigeration systems. Kilicarslan and Hosoz (2010) applied second-law analysis to a cascade refrigeration system using various refrigerant pairs, namely R152a-R23, R290-R23, R507-R23, R234a-R23, R717-R23 and R404a-R23; whereas Arora and Kaushik (2008); Oruç and Devecioğlu (2015); Yataganbaba et al. (2015) examined alternative refrigerants such as R502, R404A, R507A, R417A, R424A, R1234yf, and R1234ze to replace refrigerants harmful to the environment (*i.e.*, R22 and R134a) using exergy analysis. As for vapor compression refrigeration systems, Ahamed et al. (2011) reviewed studies on exergy analysis for vapor compression refrigeration systems and found that

irreversibilities can be reduced by condenser subcooling of up to 5 °C and reducing the temperature difference between the external fluid temperatures and the evaporating and condensing temperatures. They showed that the major portion of irreversibilities were intrinsic to the compressor, and these could be reduced by maintaining compressor discharge and suction temperatures to be within 65 and 14 °C, respectively. Bridges et al. (2001) performed a second-law analysis to quantify the irreversibilities associated with components in a household refrigerator with a volume of 18 ft³ and a split-system air conditioner with a capacity of 3 RT. They identified the potential in individual components to improve the overall exergetic efficiency of the system. The results revealed that the proportion of irreversibilities inherent to the components of the refrigerator followed the sequence; compressor, condenser, and then evaporator; whereas for the air conditioner unit, the evaporator ranked first, then the condenser and the compressor. Lee (2010) applied irreversibility analysis to data obtained from a modified R22 water-cooled screw liquid chiller with a cooling capacity of 100 RT. The analytical results showed that the percentages of the irreversibility associated with the components followed the order; compressor 38% to 47%, followed by condenser 22% to 27%, and then evaporator 17% to 23%.

The works cited above show that the application of a second-law analysis to a military Environmental Control Unit (ECU) is still lacking. The purpose of this study is to develop a methodology, based on second-law analysis, to evaluate the irreversibilities within the components of an ECU, and to identify the potential in each component to contribute to the exergetic efficiency of the overall system in high temperature ambient conditions. Three ECUs, 1.5, 3 and 5 tons of refrigeration, are tested at high ambient condition to confirm the model developed herein. The ECUs are packaged air conditioners that have a scroll type compressor, a micro-channel type condenser, a thermostatic expansion valve, and a fin-and-tube type evaporator. The 1.5 RT and 5 RT units have a hot-gas by-pass circuit and use R407C as a refrigerant, while the 3 RT unit uses R410A. Comparisons were made to provide a clear direction of how to increase the system exergetic efficiency of the Environmental Control Unit.

2. SECOND-LAW ANALYSIS

2.1 Thermodynamic Modeling

The actual vapor compression refrigeration cycle consists of several components, such as a compressor, a condenser, an expansion device, an evaporator and connecting tubes. It differs from the ideal vapor compression refrigeration cycle in several ways, mostly due to the irreversibility associated with various components. In the actual refrigeration cycle, two common sources of irreversibility are fluid friction, which causes pressure drop, and heat transfer across a finite temperature difference.

Figure 1 shows each component of a vapor compression system indicated by control volumes that experience steady-flow processes. Cengel and Boles (2002) gives mathematical expressions for the first and second laws of thermodynamics for a steady-flow process as follows:

$$\sum_{i=0}^{n} \dot{Q}_{i} - \dot{W} + \sum_{in} \dot{m} \left(h + \frac{V^{2}}{2} + gz \right) - \sum_{out} \dot{m} \left(h + \frac{V^{2}}{2} + gz \right) = 0$$
 (1)

$$\sum_{i=0}^{n} \frac{\dot{Q}_{i}}{T_{i}} + \sum_{in} \dot{m}s - \sum_{out} \dot{m}s + \dot{S}_{gen} = 0$$
 (2)

The exergy destruction (or irreversibility) during each process can be determined using the Gouy-Stodola relation:

$$\dot{I} = T_0 \dot{S}_{gen} \tag{3}$$

The exergy (or availability) for a steady-flow process of each component is calculated from the reduced form of the general exergy balance as:

$$\sum_{i=0}^{n} \left(1 - \frac{T_0}{T_i} \right) \dot{Q}_i - \dot{W} + \sum_{in} \dot{m}\psi - \sum_{out} \dot{m}\psi - \dot{I} = 0$$
 (4)

The energy, entropy, and exergy balance can be simplified by making further assumptions for each component. The evaporator, condenser, expansion valve and connecting pipelines are assumed to conduct no work. The refrigerant undergoes an actual compression process in the compressor. The throttling process of the expansion device is assumed to be isenthalpic. The changes in kinetic and potential energy of the refrigerant within every component are negligible. Analyses on evaporator and condenser fans are excluded.

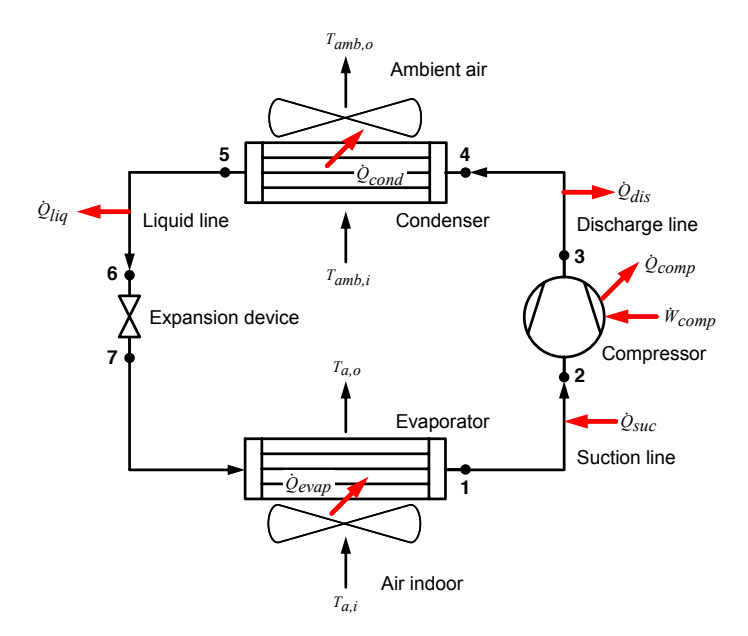


Figure 1: Schematic diagram of vapor compression system

2.2 Second-Law and Availability Analysis for ECU Components

Evaporator

The control volume of the evaporator chosen for process analysis consists of the physical structure of the evaporator, and the refrigerant and indoor airflow through the evaporator. In this process, energy is transferred from the indoor air to the refrigerant by heat. The heat transfer rate \dot{Q}_{evap} from the indoor air to the refrigerant, and the rate of entropy generation $\dot{S}_{gen,evap}$ are presented in Table 1. Notice that T_L is the sink temperature, which is the inlet bulk temperature of the indoor environment.

Component second-law efficiency ε , can be defined as the ratio of exergy recovered (or availability recovered) to the exergy supplied (or availability supplied). Therefore, the evaporator second-law efficiency ε_{evap} can be defined as the ratio of the change in indoor air exergy to the change in refrigerant exergy as shown in Table 1.

Compressor

The compression process is assumed to be non-adiabatic and irreversible. In this process, the energy transfers across the control surface include a heat loss from the compressor to its surroundings, and an external work input from the surroundings to the compressor. The rate of heat loss of the compressor \dot{Q}_{comp} and entropy generation in the compression process $\dot{S}_{gen,comp}$ are presented in Table 1. Notice that T_0 is the bulk temperature of the surroundings, \dot{W}_{comp} is the rate work input to the compressor, and \dot{m}_r is the refrigerant mass flow rate, all of which are experimentally measured. The compressor second-law efficiency ε_{comp} can be defined as the ratio of the change in flow exergy across the compressor to the actual work input as shown in Table 1.

Condenser

The control volume used to analyze the condenser encloses the entire physical structure of the condenser, and includes the refrigerant and ambient airflow through the condenser. Energy is transferred from the refrigerant to the ambient air as heat. The heat transfer rate \dot{Q}_{cond} from the refrigerant to the ambient air, and the rate of entropy generation $\dot{S}_{gen,cond}$ are shown in Table 1. Notice that T_H is the source temperature, which is the bulk temperature of outdoor ambient air at the condenser inlet. The condenser second-law efficiency ε_{cond} can be defined as the ratio of the change in ambient air exergy to the change in refrigerant exergy as shown in Table 1.

Expansion valve

The process involving the throttling device is assumed to be an isenthalpic process. Table 1 shows the rate of entropy generation $\dot{S}_{gen,cond}$, as well as the expansion valve second-law efficiency ε_{evx} which can be defined as the ratio of the outlet exergy to the inlet exergy.

Connecting Pipelines

In this work, the connecting pipelines considered include the suction, the discharge and the liquid lines, but not the line between the throttling device and the evaporator, because the throttling device and the evaporator are usually located very close to each other. The heat gained or heat lost between the pipelines and their surrounding can be expressed as shown in Table 1 as well as the associated rate of entropy generation between the pipelines and their surroundings. Moreover, Table 1 shows the second-law efficiency for the connecting pipes, which can be defined as the ratio of the outlet exergy to the inlet exergy.

Table 1: Summary of mathematical model used in second-law analysis of ECU components

Component	First-law analysis	Second-law analysis		Second-law efficiency
Evaporator	$\dot{Q}_{evap} = \dot{m}_r \left(h_1 - h_7 \right)$	$\dot{S}_{gen,evap} = \dot{m}_r \left(s_1 - s_7 \right) - \frac{\dot{Q}_{evap}}{T_L}$	$\varepsilon_{evap} = \frac{\dot{m}_{evap,a} \Delta \psi_{evap,a}}{ \dot{m}_r \Delta \psi_{evap,r} }$	$\Delta \psi_{evap,a} = h_{a,o} - h_{a,i} - T_0 (s_{a,o} - s_{a,i})$ $\Delta \psi_{evap,r} = h_1 - h_7 - T_0 (s_1 - s_7)$
Compressor	$\dot{Q}_{comp} = \dot{m}_r \left(h_3 - h_2 \right) + \dot{W}_{comp}$	$\dot{S}_{gen,comp} = \dot{m}_r \left(s_3 - s_2 \right) - \frac{\dot{Q}_{loss}}{T_0}$	$\varepsilon_{comp} = \frac{\dot{m}_r \Delta \psi_{comp}}{\dot{W}_{comp}}$	$\Delta\psi_{comp} = h_3 - h_2 - T_0 \left(s_3 - s_2 \right)$
Condenser	$\dot{Q}_{cond} = \dot{m}_r \left(h_5 - h_4 \right)$	$\dot{S}_{gen,cond} = \dot{m}_r \left(s_5 - s_4 \right) - \frac{\dot{Q}_{cond}}{T_H}$	$\varepsilon_{cond} = \frac{\dot{m}_{cond,a} \Delta \psi_{cond,a}}{ \dot{m}_r \Delta \psi_{cond,r} }$	$\Delta \psi_{cond,a} = h_{amb,o} - h_{amb,i} - T_0 (s_{amb,o} - s_{amb,i})$ $\Delta \psi_{cond,r} = h_5 - h_4 - T_0 (s_5 - s_4)$
Expansion valve	$h_6 = h_7$	$\dot{S}_{gen,exv} = \dot{m}_r \left(s_7 - s_6 \right)$	$\varepsilon_{exv} = \frac{\psi_{exv,o}}{\psi_{exv,i}}$	$\psi_{exv,i} = h_6 - h_0 - T_0 (s_6 - s_0)$ $\psi_{exv,o} = h_7 - h_0 - T_0 (s_7 - s_0)$
Connecting pipelines	$\begin{aligned} \dot{Q}_{suc} &= \dot{m}_r \left(h_2 - h_1 \right) \\ \dot{Q}_{dis} &= \dot{m}_r \left(h_4 - h_3 \right) \\ \dot{Q}_{liq} &= \dot{m}_r \left(h_6 - h_5 \right) \end{aligned}$	$\begin{split} \dot{S}_{gen,suc} &= \dot{m}_r \left(s_2 - s_1 \right) - \frac{\dot{Q}_{osc}}{T_0} \\ \dot{S}_{gen,dis} &= \dot{m}_r \left(s_4 - s_3 \right) - \frac{\dot{Q}_{des}}{T_0} \\ \dot{S}_{gen,liq} &= \dot{m}_r \left(s_6 - s_5 \right) - \frac{\dot{Q}_{leq}}{T_0} \end{split}$	$\begin{array}{l} \varepsilon_{suc} = \frac{\psi_{suc,o}}{\psi_{suc,i}} \\ \varepsilon_{dis} = \frac{\psi_{dis,o}}{\psi_{dis,i}} \\ \varepsilon_{liq} = \frac{\psi_{ilq,o}}{\psi_{liq,i}} \end{array}$	$\begin{array}{l} \psi_{suc,i} = h_1 - h_0 - T_0 \left(s_1 - s_0 \right) \\ \psi_{suc,o} = h_2 - h_0 - T_0 \left(s_2 - s_0 \right) \\ \psi_{dis,i} = h_3 - h_0 - T_0 \left(s_3 - s_0 \right) \\ \psi_{dis,o} = h_4 - h_0 - T_0 \left(s_4 - s_0 \right) \\ \psi_{liq,i} = h_5 - h_0 - T_0 \left(s_5 - s_0 \right) \\ \psi_{liq,o} = h_6 - h_0 - T_0 \left(s_6 - s_0 \right) \end{array}$

2.3 First- and Second-Law Efficiency of ECUs

The total exergy destruction (or irreversibility) of a vapor compression cycle is

$$\sum \dot{I}_i = T_0 \left(\dot{S}_{gen,comp} + \dot{S}_{gen,cond} + \dot{S}_{gen,exv} + \dot{S}_{gen,evap} + \dot{S}_{gen,suc} + \dot{S}_{gen,dis} + \dot{S}_{gen,liq} \right)$$
(5)

Therefore, the exergy destruction ratio for each component of vapor compression cycle can be defined as follows:

$$E_d = \frac{\dot{I}_i}{\sum \dot{I}_i} \tag{6}$$

The coefficient of performance of a vapor compression cycle, defined based on the first law of thermodynamics by:

$$COP_c = \frac{\dot{Q}_{evap}}{\dot{W}_{comp}} \tag{7}$$

The second-law efficiency ε , can be defined as the ratio of the actual COP to the maximum possible COP under the same operating conditions:

$$\varepsilon_c = \frac{\text{COP}_c}{\text{COP}_{rev}} \tag{8}$$

where COP_{rev} is defined as

$$COP_{rev} = \frac{T_L}{T_H - T_L} \tag{9}$$

where T_H and T_L are the absolute source and sink temperatures, respectively.

3. EXPERIMENTAL METHODOLOGY

3.1 ECUs and Experimental Setup

Three Environmental Control Units, abbreviated as 18K, 36K and 60K ECUs, were tested under the same extreme conditions in side-by-side psychrometric chambers to validate the effectiveness of the second-law analysis. The 18K

ECU uses R407C as a working refrigerant and has a rated capacity of 1.5 RT (18,000 Btu/hr). Figure 2 illustrates the system schematic. The compressor is a hermetic scroll type compressor. The condenser is based on a micro-channel design made of aluminum and treated with corrosion resistant clad material. The throttling device is an externally equalized thermostatic expansion valve. The evaporator is a fin-and-tube type heat exchanger, and made of copper tubes E-coated for corrosion protection. The fins are made of aluminum and E-coated as well. There is also a hot-gas by-pass circuit that allows the system to continue to run even if the thermostat is satisfied. The isolation ball valves are used to deactivate the hot-gas and the de-superheating valves and therefore, only four components are active all time. The 60K ECU is of the same type as the 18K ECU except that it is rated for a cooling capacity of 5 RT (60,000 Btu/hr). The 36K ECU is of the same type as the 18K ECU except that the 36K ECU has no bypass circuit and it is rated for a cooling capacity of 3 RT (36,000 Btu/hr). It has two condenser fans and uses R410A as a refrigerant. The 18K, 36K, and 60K ECUs were charged with 1.48 kg (3.27 lb), 2.36 kg (5.21 lb), and 2.98 kg (6.56 lb), respectively. The 18K, 36K, and 60K ECUs had scroll type compressor with a displacement of 7.14, 8.82, and 19.53 m³/h, respectively.

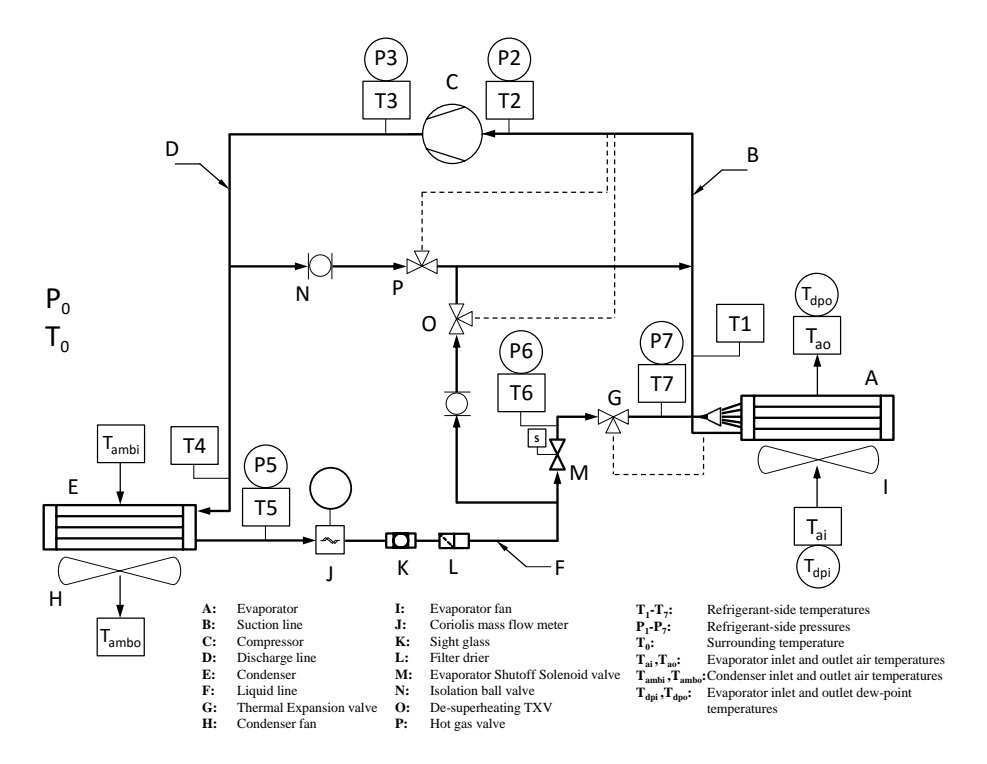


Figure 2: The measured points of ECUs

Two psychrometric chambers were used to conduct the ECU performance tests. These chambers supply uniform air flow with temperature and humidity maintained within ± 0.55 °C and $\pm 0.5\%$, respectively, of their set-points. The following parameters were measured: temperatures and pressures at the inlet and outlet of all components, refrigerant flow rate, air humidity at the inlet and outlet of the evaporator, and power consumption. All measuring instrumentation conformed to the requirements of ANSI/AHRI Standard 210/240 (Standard, 2008). Figure 2 presents the position of the mounting of each measuring instrument, while Table 3 states the accuracy of the respective instruments. Due to the compactness of the units, it is assumed that the tube-side pressure is constant in the suction and discharge lines.

3.2 Experimental Methods

The experiments were conducted in a pair of psychrometric chambers that simulate indoor and outdoor conditions, with the ECU positioned in the outdoor chamber. The testing conditions required maintaining the dry-bulb temperature of indoor air at evaporator inlet at 32.2 °C (90 °F) and wet-bulb temperature of 29.4 °C (85 °F), and maintaining the dry-bulb temperature of the ambient air at inlet to the condenser at 51.7 °C (125 °F) and wet-bulb temperature at 23.9 °C (75 °F). Once the ECU reached steady state and had been kept running for more than one hour, data measurements were taken every two seconds for 15 minutes. The averages values of the measured data were used in the second-law analysis to quantify irreversibility. In each test, the energy balance between the air-side and refrigerant-side was

Table 2: Measurement instrument and accuracy

Physical parameter	Instrument	Range	Accuracy
Temperature	Stainless steel T-type	−250-350 °C	±0.5 °C
Pressure	Pressure transducer	0-1750, 0-3500, 0-7000 kPa	$\pm 0.08\%$ FS
Air humidity	Hygrometer chilled mirror	−20-85 °C, 0-95%	±0.2 °C
Refrigerant flow rate	Coriolis flow meter	0-2720 kg/hr	$\pm 0.2\%$
Power consumption	Power transducer	0-45 kW	$\pm 0.25\%$ FS

within 6% per ANSI/AHRI Standard 210/240 (Standard, 2008). Each ECU test was carefully performed at the same temperatures in the outdoor and indoor psychrometric chambers to increase the reliability of the test results.

4. RESULTS AND DISCUSSION

The mathematical model in this work was developed using Engineering Equation Solver EES (Klein and Alvarado, 2014). The state parameters given as input to the simulation model are chosen to be those measured during the performance test. EES is used to compute the thermodynamics state properties as well.

Table 3 presents the measured temperature and pressure data at each state point in the three ECUs, from which the enthalpy, entropy and other thermodynamic properties at each state could be determined. Figure 3 illustrates a pressure-enthalpy diagram of the vapor compression refrigeration cycle of each ECU. The second-law or irreversibility analysis was computed using the data in Table 3 and the related equations presented in the mathematical section. Table 4 presents the results of the second-law analysis. Figure 4 shows the exergy destruction of each component for the three ECUs, while Figure 5 illustrates the exergy destruction ratio of components for the three ECUs. The following sections discuss the analytical results for the three ECUs that are based on Table 4 and Figures 3 to 5.

Table 3: Thermodynamics properties measured and calculated at various state points

Unit	State	Pressure kPa	Temperature °C	Enthalpy kJ/kg	Entropy kJ/kg-K	Specific volume m³/kg	Description
	1	655.8	16.59	420.4	1.785	0.037150	Evaporator outlet
	2	655.8	17.92	421.7	1.790	0.037430	Compressor inlet
	3	3108	111	486.2	1.857	0.009306	Compressor outlet
18K	4	3108	110	485.1	1.854	0.009252	Condenser inlet
	5	3095	60.57	295.6	1.307	0.001048	Condenser outlet
	6	3080	60.47	295.5	1.307	0.001047	Expansion valve inlet
	7	975	19.76	295.6	1.331	0.010040	Evaporator inlet
	1	1069	18.58	434.5	1.829	0.025910	Evaporator outlet
	2	1069	19.14	435.1	1.831	0.026010	Compressor inlet
	3	4363	110.1	492.6	1.875	0.007530	Compressor outlet
36K	4	4363	95.26	471.5	1.819	0.006708	Condenser inlet
	5	4316	58.67	302.3	1.326	0.001165	Condenser outlet
	6	4301	58.57	302.1	1.326	0.001165	Expansion valve inlet
	7	1308	16.4	302.4	1.355	0.008100	Evaporator inlet
	1	625.3	20.75	425.2	1.806	0.040160	Evaporator outlet
	2	625.3	25.75	430	1.822	0.041210	Compressor inlet
	3	3213	111.9	486.2	1.855	0.008957	Compressor outlet
60K	4	3213	110.2	484	1.849	0.008862	Condenser inlet
	5	3145	61.2	296.8	1.311	0.001052	Condenser outlet
	6	3130	61.1	296.6	1.31	0.001052	Expansion valve inlet
	7	1072	23.05	296.8	1.329	0.008100	Evaporator inlet

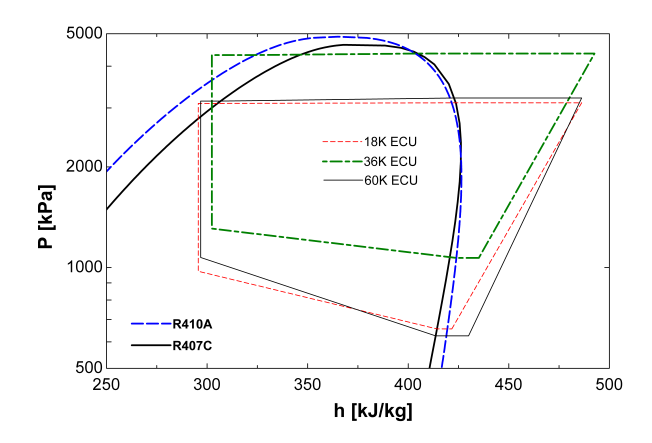


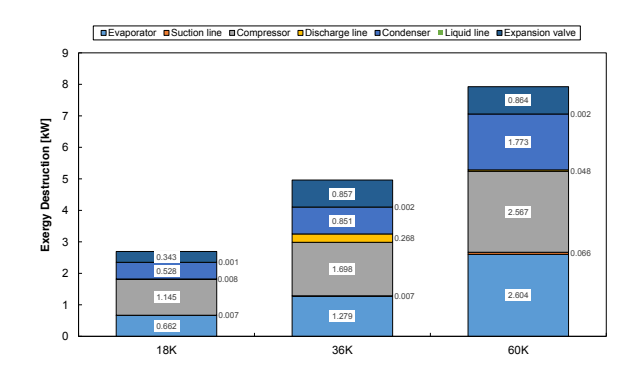
Figure 3: Pressure-enthalpy diagram of ECUs under the same testing conditions

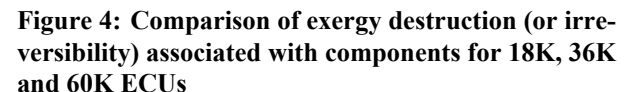
Table 4: Results of first-law and second-law analysis of three ECUs

		First-law analysis		Second-law analysis					
Unit	Component	Ż	W	COP_c	\dot{S}_{gen}	İ	E_d	ε	ε_c
		kW	kW	-	kW/K	kW	%	-	-
	Evaporator	5.585	0		0.002037	0.6617	24.57	0.4879	0.1166
	Suction line	0.0589	0		0.00002148	0.006978	0.2591	0.9973	
	Compressor	-0.1617	3.049		0.003524	1.145	42.5	0.6246	
18K	Discharge line	-0.0534	0	1.832	0.00002521	0.008187	0.3039	0.9982	
	Condenser	-8.471	0		0.001626	0.528	19.6	0.0969	
	Liquid line	-0.007499	0		0.000002718	0.000883	0.03278	0.9979	
	Expansion valve	0	0		0.001056	0.3431	12.74	0.9137	
	Total	-3.049	3.049		0.008293	2.694	100.00	-	
	Evaporator	12.42	0	2.159	0.003938	1.279	25.78	0.4995	0.1375
	Suction line	0.05812	0		0.0000201	0.00653	0.1316	0.9992	
	Compressor	-0.3604	5.753		0.005227	1.698	34.22	0.7049	
36K	Discharge line	-1.979	0		0.0008241	0.2677	5.395	0.9779	
	Condenser	-15.88	0		0.002621	0.8512	17.15	0.0752	
	Liquid line	-0.01774	0		0.000006087	0.001977	0.03984	0.9757	
	Expansion valve	0	0		0.00264	0.8574	17.28	0.9221	
	Total	-5.753	5.753		0.01528	4.962	100.00	-	
	Evaporator	18.43	0	2.026	0.00802	2.605	32.88	0.4554	0.129
60K	Suction line	0.6911	0		0.00021041	0.06628	0.8366	0.9919	
	Compressor	-1.04	9.096		0.007904	2.567	32.4	0.7178	
	Discharge line	-0.3129	0		0.0001489	0.04836	0.6104	0.9967	
	Condenser	-26.84	0		0.005458	1.773	22.37	0.0478	
	Liquid line	-0.02409	0		0.00000887	0.002881	0.03636	0.9962	
	Expansion valve	0	0		0.002649	0.8605	10.86	0.9329	
	Total	-9.096	9.096		0.02439	7.923	100.00	-	

4.1 Performance of the 18K ECU

The result of the first- and second-law analyses of the 18K ECU are shown in Table 4. The COP_c is 1.83. Additionally, the rate of entropy generation is greatest in the compressor, followed by the evaporator and condenser in that order, with an entropy generation of 0.003524, 0.002037 and 0.001626 kW/K, respectively. Figure 4 shows the comparison of irreversibility inherent to each component for the 18K, 36K and 60K ECUs. In the case of 18K ECU, the largest rate of irreversibility is present within the compressor (1.145 kW), followed by the evaporator with 0.6617 kW and then the condenser with 0.528 kW.





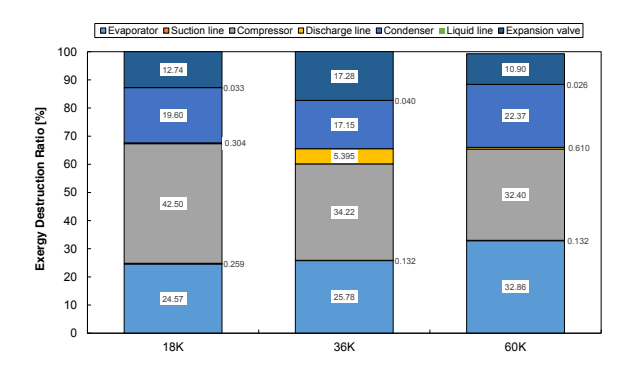


Figure 5: Comparison of exergy destruction (or irreversibility) ratio associated with components for 18K, 36K and 60K ECUs

Figure 5 illustrates that the irreversibility ratios were 42.5%, 24.6% and 19.6% for the compressor, the evaporator and the condenser, respectively. The sum of the exergy destruction ratios of these three components approximately equals 87%. Clearly, the compressor should be considered first when improving the exergetic efficiency of the 18K ECU. The second-law efficiency ε , at component level, is low for the condenser, evaporator and compressor with values of 9.7%, 48.8% and 62.5%, respectively. The exergy recovered in the condenser is small because of the high ambient temperature, *i.e.*, 51.7 °C (125 °F) which results in a low second-law efficiency. The overall second-law efficiency ε_c of the unit is 11.7%.

4.2 Performance of the 36K ECU

As shown in Table 4, the analytical results for the 36K ECU indicate a COP_c of 2.16. The rate of entropy generation for each component follows the order of compressor, evaporator, expansion valve then condenser, with values of 0.005227, 0.003938, 0.00264 and 0.002621 kW/K, respectively.

Figure 3 compares the refrigeration cycles of the three ECUs and indicates that the 36K ECU exhibited a higher condensing temperature and discharge temperature than that of the other two ECUs. The 36K ECU has the same construction as the other ECUs except that it uses R410A as a refrigerant. Notice from the figure that the pressure measurements were taken before the evaporator distributor, which explains the steep degradation in pressure drop.

Examining Figures 4 and 5, the highest irreversibility is present within the compressor at 1.689 kW, followed by that in the evaporator at 1.278 kW, then that in the expansion valve at 0.8574 kW, and finally that in the condenser at 0.8512 kW. The irreversibility ratios for individual component are 34.2%, 25.8%, 17.3%, and 17.2%, respectively. As in 18K ECU, the compressor should be considered first to improve the exergetic efficiency of the unit.

Similar to the 18K ECU, the component second-law efficiencies ε of the 36K ECU are relatively low for the condenser, followed by the evaporator, then the compressor, with respective values of 7.5%, 50% and 70.5%. As in the 18K ECU, the exergy recovered in the condenser of the 36K ECU is small due to the high ambient temperature. Notice that in Figure 4 and 5, the discharge line exhibits relatively high irreversibility because of the higher entropy generation caused by heat transfer due to the additional condenser fan. Consequently, the higher heat transfer rate reduces the entropy generation of the condenser and thus lowers the condenser irreversibility. The overall second-law efficiency ε_c of the 36K ECU is 13.8%.

4.3 Performance of the 60K ECU

Table 3 shows the analytical results of the 60K ECU, which has a COP_c of 2.03. Unlike the 18K and 36K ECUs, the rate of entropy generation within each component of the 60K ECU follows the order of the evaporator, the compressor, and then the condenser, with respective values of 0.00801, 0.0079, and 0.00265 kW/K.

Figure 4 illustrates that the highest component irreversibility of the 60K ECU is associated with the evaporator, followed by the compressor, and then the condenser, with respective values of 2.605, 2.567, and 1.773 kW. As for the corresponding irreversibility ratios, as shown in Figure 5, the associated ratios for the evaporator, compressor, and

condenser are 32.9%, 32.4% and 22.4%, respectively. The sum of the exergy destruction ratios of these three components equals approximately 88%. The pressure drop associated with the distributor in the evaporator of 60K ECU, as shown in Figure 3, results in relatively higher irreversibility. Unlike the 18K and 36K ECUs, both the evaporator and the compressor of the 60K ECU should be considered to increase the exergetic efficiency of the unit.

As was the case for the 18K and 36K ECUs, the condenser of the 60K ECU has the lowest second-law efficiency ε , followed by the evaporator, and then the compressor with 4.8%, 45.5% and 71.8%, respectively. Again, the exergy recovered in the condenser of this unit is small due to the high ambient temperature. The overall second-law efficiency ε_c of the 60K ECU is 12.9%.

5. CONCLUSIONS

This paper presented second-law analyses of three military Environmental Control Units (ECUs) to identify the contribution of each component to the overall irreversibilities of the units. This way, the components in highest need of improvement in energy efficiency can be identified. The three ECUs were experimentally investigated at high ambient condition and comparisons between the individual components were made to provide a clear direction of how to increase the exergetic efficiency of the ECUs. The results yield the following conclusions:

- The exergy destruction (or irreversibility) associated with each component in the tested ECUs follow the sequence, compressor associated with 32.4% to 42.5% of the total system irreversibility, followed by the evaporator associated with 24.6% to 32.9%, followed by the condenser associated with 19.6% to 22.4%.
- The analytical results indicate that compressor should be considered first in increasing the exergetic efficiency of all ECUs; whereas in 60K ECU, evaporator should also be considered.
- An additional condenser fan helps the 36K ECU reducing the exergy destruction (or irreversibility) associated with the condenser, but increases the irreversibility of the discharge line.
- A second-law analysis helps identifying components with higher exergy destruction (or irreversibility) and clarifying which component modification can increase the exergetic efficiency of any ECU operating in high temperature ambient conditions.

NOMENCLATURE

E_d	exergy destruction ratio	(-)	Subscripts	
g	gravity constant	(m/s^2)	a	air
h	enthalpy	(kJ/kg)	amb	ambient
İ	exergy destruction	(kW)	c	cycle
m	mass flow rate	(kg/s)	comp	compressor
P	pressure	(kPa)	cond	condenser
\dot{Q}	heat rate	(kW)	dis	discharge
S	entropy	(kJ/kg-K)	evap	evaporator
\dot{S}_{gen}	entropy generation	(kW/K)	exv	expansion valve
T	temperature	(°C)	H	high
V	velocity	(m/s)	i	inlet
\dot{W}	power	(kW)	0	outlet
\boldsymbol{z}	elevation	(m)	liq	liquid
COP	coefficient of performance	(-)	L	low
ECU	environmental control unit	(-)	r	refrigerant
RT	refrigeration tons	(-)	rev	reversible
Greek symbols			suc	suction
Ψ	exergy	(kJ/kg)	0	surrounding
ε	second-law efficiency	(-)	$1, 2, 3 \dots, 7$	components

REFERENCES

- Ahamed, J. U., Saidur, R., and Masjuki, H. H. (2011). A review on exergy analysis of vapor compression refrigeration system. *Renewable and Sustainable Energy Reviews*, 15(3):1593–1600.
- Arora, A. and Kaushik, S. C. (2008). Theoretical analysis of a vapour compression refrigeration system with R502, R404A and R507A. *International Journal of Refrigeration*, 31(6):998–1005.
- Bejan, A. (1988). Advanced engineering thermodynamics. John Wiley & Sons, Inc.
- Bridges, B. D., Harshbarger, D. S., and Bullard, C. W. (2001). Second law analysis of refrigerators and air conditioners. *ASHRAE Transactions*, 107:644.
- Cengel, Y. A. and Boles, M. A. (2002). *Thermodynamics: an engineering approach*. McGraw-Hill New York, 4th edition.
- Dincer, I. and Rosen, M. A. (2015). Exergy Analysis of Heating, Refrigerating and Air Conditioning. Elsevier.
- Fartaj, A., Ting, D. S. K., and Yang, W. W. (2004). Second law analysis of the transcritical CO2 refrigeration cycle. *Energy Conversion and Management*, 45(13-14):2269–2281.
- Kilicarslan, A. and Hosoz, M. (2010). Energy and irreversibility analysis of a cascade refrigeration system for various refrigerant couples. *Energy Conversion and Management*, 51(12):2947–2954.
- Klein, S. and Alvarado, F. (2014). Engineering equation solver, academic commercial version 9.698-3d. *F-Chart Software, Madison, WI*.
- Lee, T. S. (2010). Second-Law analysis to improve the energy efficiency of screw liquid chillers. *Entropy*, 12(3):375–389
- Meunier, F., Poyelle, F., and LeVan, M. D. (1997). Second-law analysis of adsorptive refrigeration cycles: The role of thermal coupling entropy production. *Applied Thermal Engineering*, 17(1):43–55.
- Moran, M. J., Shapiro, H. N., Boettner, D. D., and Bailey, M. B. (2010). *Fundamentals of engineering thermodynamics*. John Wiley & D. Sons.
- Oruç, V. and Devecioğlu, A. G. (2015). Thermodynamic performance of air conditioners working with R417A and R424A as alternatives to R22. *International Journal of Refrigeration*, 55:120–128.
- Şencan, A., Yakut, K. A., and Kalogirou, S. A. (2005). Exergy analysis of lithium bromide/water absorption systems. *Renewable Energy*, 30(5):645–657.
- Standard, A. (2008). ANSI/AHRI Standard 210/240. Performance rating of unitary A/C and air-source heat pump equipment.
- Xu, X. X., Liu, C., Fu, X., Gao, H., and Li, Y. (2015). Energy and exergy analyses of a modified combined cooling, heating, and power system using supercritical CO2. *Energy*, 86:414–422.
- Yataganbaba, A., Kilicarslan, A., and Kurtbas, I. (2015). Exergy analysis of R1234yf and R1234ze as R134a replacements in a two evaporator vapour compression refrigeration system. *International Journal of Refrigeration*, 60:26–37.

ACKNOWLEDGEMENT

The authors would like to thank Adams Communication & Engineering Technology (ACET) for sponsoring the ECU project.